Journal of Sound and Vibration (2000) **234**(3), 427–439
doi:10.1006/jsvi.1999.2889, available online at http://www.idealibrary.com on IDEAL®

LOCAL ACTIVE SOUND CONTROL USING 2-NORM AND ∞-NORM PRESSURE MINIMIZATION

W.-K. Tseng, B. Rafaely and S. J. Elliott

Institute of Sound and Vibration Research, University of Southampton, Southampton SO17 1BJ, England

(*Received* 26 *July* 1999, *and in final form* 21 *December* 1999)

This paper presents a method of designing active noise control systems to generate zones of quiet in which a new approach was employed, involving 2-norm or ∞-norm pressure minimization in the quiet zone. This is in contrast to the conventional design method, where the acoustic pressure or the acoustic pressure and particle velocity are set to zero at given cancellation points, with no direct control on the size and shape of the quiet zones. It is shown that larger zones of quiet are obtained using this new approach, with better control over the shape of the zones of quiet.

1. INTRODUCTION

Traditional methods of passive noise control used enclosures and barriers surrounding the noise source to attenuate the noise around the source. However, passive techniques do not work well at low frequencies. In the last decade, active noise control (ANC) has been developed significantly to deal with low-frequency noise. It works by introducing secondary sources which produce "antinoise" waves to cancel the primary (unwanted) noise. The most desirable noise control result would be the attenuation of sound pressure in all directions in space or in an entire enclosure. Unfortunately, this global control can only be achieved when the primary sources and the secondary sources are closely located or when only few significant modes exist in an enclosure [1]. In practical applications, these conditions may not be satisfied, and the preferred choice for active noise control may be to cancel the sound pressure in some restricted volume and thus produce quiet zones. This control strategy is called local control and generally involves the use of secondary sources to cancel the pressure at a closely spaced error microphone. Local active noise control can be applied inside automobiles and aircraft to cancel the noise near a listener's ear.

A conventional method of generating a zone of quiet is to cancel the pressure at a point using a single secondary source. The shape of the quiet zone created by using a single cancellation point and a monopole source is a shell-like volume surrounding the secondary source at low frequencies, and a smaller volume surrounding the cancellation point at higher frequencies [2]. The resulting on-axis pressure around the cancellation point is determined by the nearfield characteristics of the secondary source, which limits the diameter of the zone of quiet so that it is less than one-tenth of a wavelength at the excitation frequency [3–5].

An alternative method in local active noise control is to cancel the pressure or the pressure and particle velocity at a number of points using multi-pole secondary sources. Cancelling the pressure at several cancellation points could produce larger zones of quiet [6–8], however, the optimal spacing between the cancellation points is dependent on the

0022-460X/00/280427 + 13 $35.00/0

wavelength and therefore varies with frequency. Cancelling the pressure and particle velocity has been shown to considerably increase the extension of the zone of quiet compared to simply cancelling the pressure [9–11].

All the approaches described above used "cancellation points" in the process of calculating the best secondary field, i.e., the pressure (or particle velocity) at discrete points in the quiet zones was driven to zero, thus producing lower total pressure near the cancellation points, but with no control over the shape of the quiet zones. In this work, a different approach is used to calculate the secondary field. First, the desired spatial extent of zone of quiet is defined. Then, the secondary field is chosen which minimizes the pressure at the quiet zone. Both space-averaged pressure (2-norm) and maximum pressure (∞-norm) are used as criteria for pressure minimization. This approach will not necessarily produce cancellation points, i.e., points where the total pressure is zero. However, due to the optimal design, the best overall attenuation of sound is achieved in the desired region.

The paper is presented as follows: in section 2, the formulation of 2- and ∞-norm pressure minimization is introduced. The methods of designing quiet zones for a diffuse primary field are described in section 3, and the quiet zone simulations are presented in section 4. The paper is then concluded in section 5.

2. FORMULATION OF 2- AND ∞-NORM PRESSURE MINIMIZATION

In this section, the formulation of the 2- and the ∞-norm pressure minimization is presented, which is then used for local sound control in a diffuse primary field.

In general, the 2-norm of a scalar function $g(x)$ is defined as [12]

$$\| g(x) \|_2 = \left(\int_{-\infty}^{\infty} |g(x)|^2 \, \mathrm{d}x \right)^{1/2}. \tag{1}$$

In this work, the pressure is minimized over an area, and it is a function of two spatial variables, x and y, so a double integral over x and y would be used. Also, the continuous function of pressure is approximated at a finite number of discrete points with spacing much smaller than a wavelength, forming a matrix $\mathbf{P}$ of pressure values. The 2-norm of the pressure matrix is now defined as

$$\| \mathbf{P} \|_2^2 = \sum_{i,j} |p(x_i, y_j)|^2, \tag{2}$$

where $p(x_i, y_j)$ is the complex acoustic pressure at position (x_i, y_i) at a single excitation frequency and corresponds to the element (i, j) in matrix $\mathbf{P}$. In active control, the total pressure $\mathbf{P}$ is composed of primary and secondary components, $\mathbf{P}_p$ and $\mathbf{P}_s$, respectively, such that $\mathbf{P} = \mathbf{P}_p + \mathbf{P}_s$. The optimal secondary field $\mathbf{P}_s$, which minimizes the 2-norm of the total pressure in a given area can be calculated by minimizing the sum of squared pressure as follows:

$$\min_{\mathbf{P}_s} \| \mathbf{P} \|_2^2 = \min_{\mathbf{P}_s} \| \mathbf{P}_p + \mathbf{P}_s \|_2^2 = \min_{\mathbf{P}_s} \sum_{i,j} |p_p(x_i, y_j) + p_s(x_i, y_j)|^2. \tag{3}$$

The 2-norm quiet zone minimization is performed by first defining the area of the quiet zone, and then computing the strengths of the secondary sources which will minimize the sum of squared total pressure in the quiet zone. This approach ensure maximum overall reduction in the sound level over the area of the quiet zone.

The ∞-norm of a scalar function $g(x)$ is defined as [12]

$$\| g(x) \|_\infty = \sup_x |g(x)|, \tag{4}$$

where sup is the lowest upper limit. The ∞-norm corresponds to the peak magnitude of the function.

If $p(x, y)$ is evaluated at discrete points to form again the matrix $\mathbf{P}$ and the ∞-norm is approximated by the matrix max-norm:

$$\| \mathbf{P} \|_\infty = \max_{i,j} |p(x_i, y_j)|, \tag{5}$$

then the optimal secondary field, $\mathbf{P}_s$, which minimizes the maximum value of the total pressure, $\mathbf{P}$, can be found by

$$\min_{\mathbf{P}_s} \| \mathbf{P} \|_\infty = \min_{\mathbf{P}_s} \| \mathbf{P}_p + \mathbf{P}_s \|_\infty = \min_{\mathbf{P}_s} \max_{i,j} |p_p(x_i, y_j) + p_s(x_i, y_j)|. \tag{6}$$

The ∞-norm quiet zone minimization will result in minimal peak of the pressure at the quiet zone. This approach ensures that the pressure in the quiet zone has the lowest possible maximum value [13].

3. METHODS OF DESIGNING QUIET ZONES

In this section, we present the wave model of a pure tone diffuse sound field used in the quiet zone simulations to generate the primary field, and the formulations for the design of the quiet zones using 2- and ∞-norm pressure minimization.

In this work, the primary field is assumed to be diffuse and comprised of many propagating plane waves with random amplitudes and phases, arriving from uniformly distributed directions. Although the waves occupy a three-dimensional space, the quiet zone analysis is performed, for simplicity, over a two-dimensional area. Therefore, the pressure at the point (x_0, y_0) on the x–y plane due to a single incident plane wave travelling along line r as shown in Figure 1 can be expressed as [14]

$$p(x_0, y_0) = (a + \mathrm{j}b) \exp(-\mathrm{j}k(y_0 \sin\theta_K \sin\varphi_L + x_0 \sin\theta_K \cos\varphi_L)), \tag{7}$$

where $(a + \mathrm{j}b)$ accounts for the amplitude and phase of this incident plane wave, k is the acoustic wave number, θ_K is the angle between the direction of plane wave propagation and the z-axis, and φ_L is the angle between the direction of the plane wave propagation projected on the x–y plane and the x-axis. In our study, we chose 72 such incident plane waves together with random amplitudes and phases to generate an approximation of a diffuse sound field in order to be consistent with that of previous work [10, 11]. The diffuse sound field was therefore generated by adding together the contributions of 12 plane waves in the azimuthal directions (corresponding to azimuthal angles $\varphi_L = L \times 30^\circ$, $L = 1, 2, 3, \ldots, 12$) for each of six vertical incident directions (corresponding to vertical angles $\theta_K = K \times 30^\circ$ for $K = 1, 2, 3, \ldots, 6$). The net pressure at the point (x_0, y_0) on the x–y

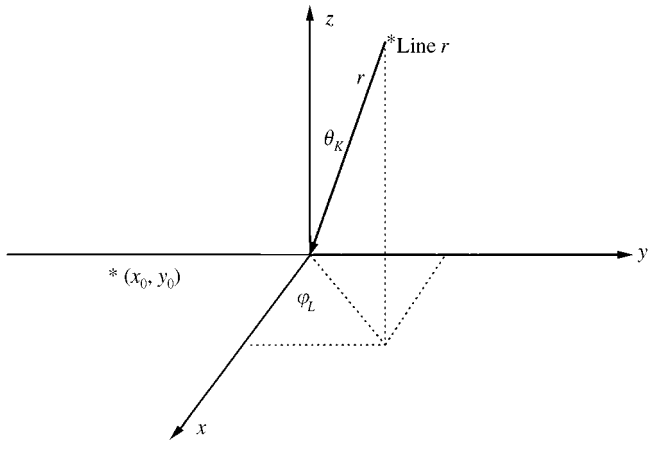

Figure 1. Definition of spherical co-ordinates r, θ_K, φ_L for an incident plane wave travelling along the direction of line r.

plane due to the superposition of these 72 plane waves was then calculated from equation (7) as follows [14]:

$$P_p(x_0, y_0) = \sum_{K=1}^{K_{\max}} \sum_{L=1}^{L_{\max}} (a_{KL} + \mathrm{j}b_{KL}) \sin\theta_K \exp(\mathrm{j}k(x_0 \sin\theta_K \cos\varphi_L + y_0 \sin\theta_k \sin\varphi_L)), \quad (8)$$

in which both the real and imaginary parts of the complex pressure are chosen from a random population with Gaussian distribution $N(0, 1)$. Equation (8) was used to generate diffuse primary sound fields in the simulations presented below. The computation of the average diffuse field zone of quiet at a given frequency is based on an ensemble of 50 samples of diffuse fields calculated over a grid of 131×131 points in the x–y plane. The primary field samples are calculated once and then used in the calculation of the various controlled fields (equation (10)).

The design of quiet zones using 2- and ∞-norm minimization is studied in this work by assuming that the secondary field is produced by monopole sources. Although this is not an accurate model of practical sources, it simplifies the design procedure and assists comparison with previous studies. Since the simulations described below involve one, two or three secondary sources, we start, for simplicity, by considering one secondary source located at the origin. The total acoustic pressure at a field point a distance r from the origin due to both the diffuse primary field and the single secondary monopole can be expressed as

$$p_T(x, y) = p_p(x, y) + A \frac{\mathrm{e}^{-\mathrm{j}kr(x, y)}}{r(x, y)}, \quad (9)$$

where $p_p(x, y)$ is the complex pressure due to the diffuse primary field at the point (x, y), $A = \mathrm{j}\omega\rho_0 q/4\pi$, with $\omega = 2\pi f$ the angular frequency, ρ_0 is the density of the air, q is the source strength, $r(x, y) = \sqrt{(x^2 + y^2)}$ is the distance between the field point (x, y) and the secondary monopole, and k is the acoustic wavenumber.

For two secondary monopoles which are a distance d apart in the x direction as shown in Figure 2, the total acoustic pressure at a field point a distance r from the origin due to both

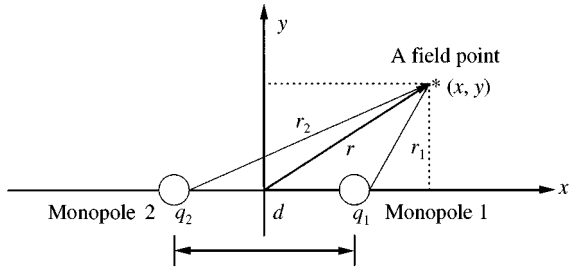

Figure 2. Configuration of active noise control using two secondary monopole sources.

the diffuse primary field and the two secondary monopoles can be expressed as

$$p_T(x, y) = p_p(x, y) + A_1 \frac{e^{-jkr_1(x,y)}}{r_1(x, y)} + A_2 \frac{e^{-jkr_2(x,y)}}{r_2(x, y)}, \tag{10}$$

where in the term describing the first monopole, $A_1 = j\omega\rho_0 q_1/4\pi$, q_1 the source strength and $r_1(x, y) = \sqrt{(x - d/2)^2 + y^2}$ is the distance between the field point (x, y) and the secondary monopole. For the second monopole $A_2 = j\omega\rho_0 q_2/4\pi$, and $r_2(x, y) = \sqrt{(x + d/2)^2 + y^2}$ is the distance between the field point (x, y) and the secondary monopole. The results can then easily be extended for a larger number of secondary sources.

The minimization cost function for the 2-norm pressure minimization using two secondary monopoles is therefore written by substituting equation (10) into equation (3) as

$$J_2 = \sum_{i,j} |p_T(x_i, y_j)|^2 = \sum_{i,j} \left| p_p(x_i + y_j) + A_1 \frac{e^{-jkr_1(x_i,y_j)}}{r_1(x_i, y_j)} + A_2 \frac{e^{-jkr_2(x_i,y_j)}}{r_2(x_i, y_j)} \right|^2, \tag{11}$$

where $p_T(x_i, y_j)$ is the total acoustic pressure within the minimization area as described in equation (10). We can find the optimal values of the complex variables A_1 and A_2 which minimize the cost function J_2 by using the function fmins( ) in MATLAB [15], or analytically by converting equation (11) to an Hermitian quadratic form [1].

Substituting the optimal values of A_1 and A_2 into equation (10), we can calculate the controlled field, $P_T(x, y)$, for each diffuse field sample (comprised of 72 plane waves as described at the beginning of this section) generated using equation (8) at each position (x, y) in the quiet zone. The average reduction $R(x, y)$ in the 2-norm of the sound pressure in the zone of quiet for 50 samples of the diffuse field is then calculated as the ratio of the mean total (controlled) squared pressure over the 50 samples, and the mean primary squared pressure over the 50 samples, as follows:

$$R(x, y) = \frac{\overline{|P_T(x, y)|^2}}{\overline{|p_p(x, y)|^2}}. \tag{12}$$

For ∞-norm pressure minimization, the following cost function is minimized:

$$J_\infty = \max_{i,j} |p_T(x_i, y_j)| = \max_{i,j} \left| p_p(x_i, y_j) + A_1 \frac{e^{-jkr_1(x_i,y_j)}}{r_1(x_i, y_j)} + A_2 \frac{e^{-jkr_2(x_i,y_j)}}{r_2(x_i, y_j)} \right|. \tag{13}$$

This ∞-norm minimization which is a convex optimization problem, i.e., it has a unique solution [13], can be rewritten as linear minimization problem with ∞-norm constraint [16],

$$\text{i.e., minimize } \sigma, \text{ subject to the constraint } J_\infty < \sigma, \tag{14}$$

where σ is a real scalar parameter used in the optimization process.

The optimal values of A_1 and A_2 can be calculated using the function constr( ) in MATLAB [15]. The method used here to calculate the average zones of quiet is similar to that described in the 2-norm minimization procedure. In this work only two-dimensional zones of quiet were considered. The algorithm to calculate the quiet zones could be easily extended to three-dimensional zones of quiet, although the computation will be more time consuming. For the three-dimensional zones of quiet considered in this paper, the quiet zones on the x–z plane should be the same as those on the x–y plane due to the rotational symmetry of the secondary field around the x-axis.

4. QUIET ZONE SIMULATIONS

In this section, the simulated average zones of quiet created by one, two or three monopole secondary sources seeking to minimize the 2- and ∞-norm of the total acoustic pressure at various areas in a pure tone diffuse primary field are presented, and then compared to those obtained by cancelling the acoustic pressure or the acoustic pressure and particle velocity at one point.

In the first simulation, the zone of quiet created using a single monopole source is computed using 2-norm pressure minimization and compared to that created by cancelling the acoustic pressure at a single point. A pure tone diffuse primary field for $kL = 0{\cdot}6$ is generated in this case, where L is the distance from the secondary monopole to the cancellation point, k the acoustic wavenumber, and for $L = 0{\cdot}3$ m, as shown in the figures, this will correspond to an excitation frequency of 108 Hz. Figure 3 shows the 10 dB reduction contour line for 2-norm minimization (solid line) of the pressure in an area represented by the rectangular frame. Also shown is the 10 dB reduction contour line for cancelling the acoustic pressure (dash–dot line) at location $(0{\cdot}3, 0)$ marked by $+$. The secondary monopole source is represented by *. The 10 dB amplification in the acoustic pressure for 2-norm minimization (dashed line) and cancelling the pressure at a point (dotted line) are also shown in Figure 3. Figure 3 shows that the zone of quiet created by using 2-norm pressure minimization over this carefully selected area is similar to that created by cancelling the acoustic pressure at a point. This is due to the fact that the secondary field produced by a single monopole is in both cases a symmetrically decaying field, which is controlled by only two parameters, the source strength and the phase, resulting in the design method having little effect on the optimal secondary field shape in this case. The shape of the quiet zone changes with kx when cancelling the acoustic pressure at a single point, as has been discussed in previous papers [4, 14].

A single secondary monopole can only produce a symmetrically decaying field. If two secondary monopoles are used, four parameters can be adjusted and more complicated secondary fields can be produced. Therefore, larger zones of quiet could be obtained. In the next simulations, two secondary monopoles are introduced, minimizing the acoustic pressure at various areas using the 2-norm computation. The zones of quiet are then compared to those designed by cancelling the acoustic pressure and particle velocity at a point [10, 11], and those created by minimizing the acoustic pressure using the ∞-norm.

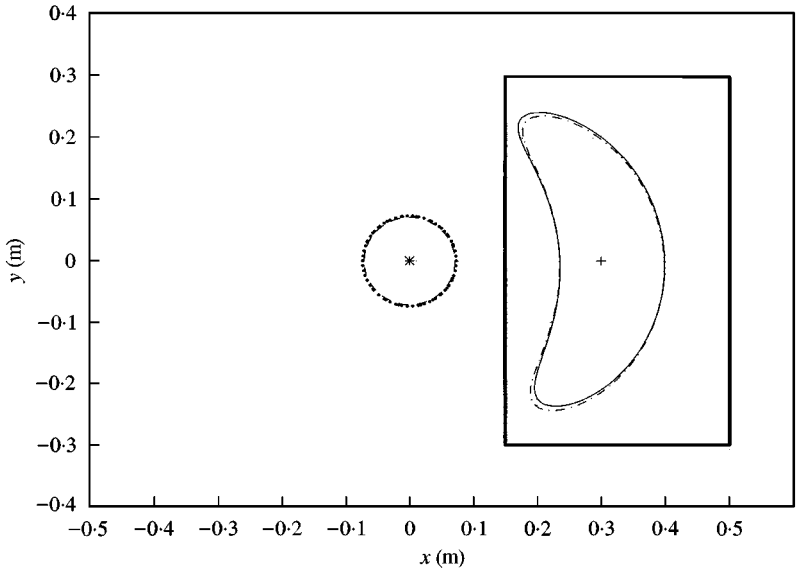

Figure 3. The 10 dB reduction contour of the average zone of quiet created by a secondary monopole source located at position (0, 0), cancelling the acoustic pressure at (0·3, 0) point (-·-·-·) and minimizing the acoustic pressure at an area represented by a bold rectangular frame using 2-norm minimization strategy (——), and the 10 dB amplification in the acoustic pressure of the diffuse primary field for cancelling the pressure at one point (·····) and for the 2-norm minimization strategy (- - - - -).

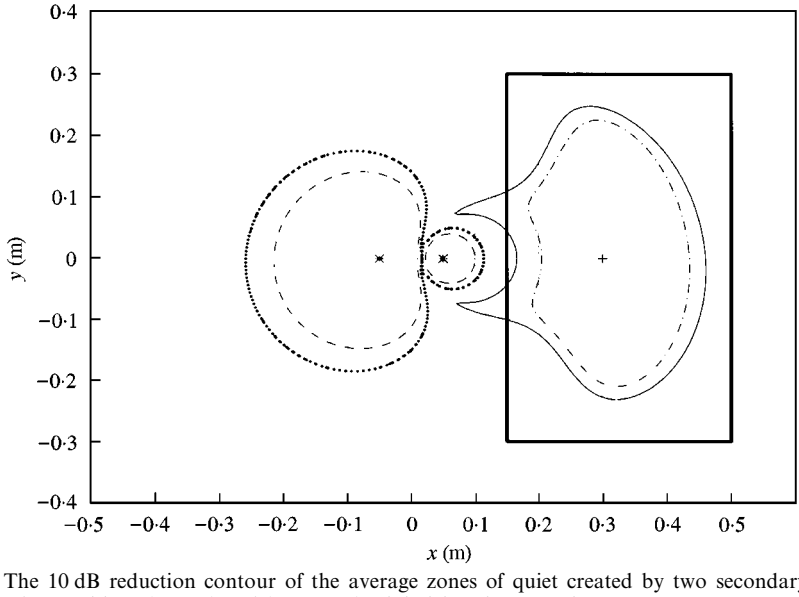

Figure 4. The 10 dB reduction contour of the average zones of quiet created by two secondary monopole sources located at positions (0·05, 0) and (− 0·05, 0) minimizing the acoustic pressure at an area represented by a bold rectangular frame using 2-norm minimization strategy (——) and cancelling the acoustic pressure and particle velocity at (0·3, 0) point (-·-·-·), and the 10 dB increase in the primary field for 2-norm minimization strategy (- - - - -) and cancelling the acoustic pressure and particle velocity at one point (. . . . .).

Figure 4 shows the 10 dB reduction contour line (solid curve) for the 2-norm minimization with the minimization area represented by the bold rectangular frame. Also shown is the 10 dB reduction contour line for the case in which the acoustic pressure and particle velocity are cancelled (dash–dot line) at location (0·3, 0). The two secondary

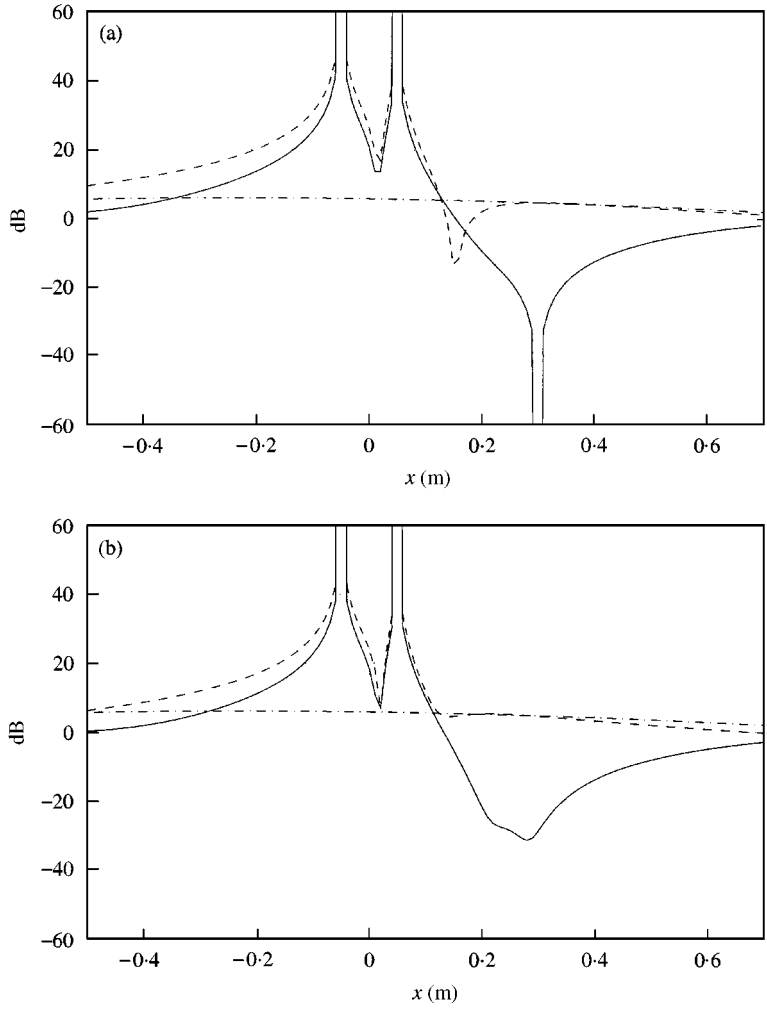

Figure 5. The mean squared pressure for primary field (-·-·-·), secondary field (- - - - -) and controlled field (——). (a) Cancelling the acoustic pressure and particle velocity at point (0·3, 0). (b) Minimizing the acoustic pressure at a rectangular area using the 2-norm minimization strategy.

monopoles located at (0·05, 0) and (− 0·05, 0) are marked by *. The 10 dB amplification is also shown for the 2-norm minimization strategy (dashed line) and for cancelling the acoustic pressure and particle velocity at one point (dotted line). Previous work showed that cancelling the acoustic pressure and particle velocity at one point by introducing two secondary monopoles created larger zones of quiet than those created by cancelling the acoustic pressure at one point only using a single secondary monopole [10, 11]. This finding is confirmed from the comparison between Figures 3 and 4. However, Figure 4 shows that minimizing the acoustic pressure over an area by using 2-norm minimization produces a larger zone enclosed by the 10 dB reduction contour compared to that created when cancelling the acoustic pressure and particle velocity at one point. This is because the two secondary monopoles in the 2-norm computation attempt to minimize the sum of squared pressure over an area, so the amplitude of the secondary field is as close as possible to the amplitude of the primary field with the opposite phase over the complete minimization area. This is in contrast to cancelling the acoustic pressure and the

particle velocity at one point, where the secondary field parameters at that point only are controlled. The size of the 10 dB amplification of the diffuse primary field is slightly smaller for 2-norm computation and the magnitude of the strength of the secondary sources, A_1 and A_2 as in equation (11), for 2-norm computation is about 3 dB smaller than those when cancelling the acoustic pressure and particle velocity. This reflects the fact that the control effort of the secondary monopoles for the 2-norm computation is smaller in this case.

In order to observe the spatial variation of the primary, secondary and controlled fields generated in the simulations above, the magnitude of the pressure fields along the x-axis only is investigated. Figure 5(a) shows the three fields for cancelling the pressure and particle velocity, and Figure 5(b) for minimizing the 2-norm of the pressure, both as presented in Figure 4. Comparing these results, we notice that the secondary and primary fields overlap around the cancellation point for the case of two secondary sources cancelling the acoustic pressure and particle velocity at this point. Therefore, the controlled field is zero at location (0·3, 0) for this case. This is since perfect cancellation is achieved at the cancellation point. However, the 2-norm minimization strategy is to minimize the sum of the squared pressure difference between the primary and secondary fields over the whole minimization area, so the controlled field is flatter than that produced by cancelling the acoustic pressure and particle velocity at one point. The zone of quiet is therefore larger in this case. Notice that no cancellation point, or a point of zero controlled pressure is obtained in this case.

The result in Figure 6 shows the contour lines of 10 dB reduction in the sound pressure level calculated using the 2-norm minimization strategy (solid line, as in Figure 4), and ∞-norm minimization strategy (dash–dot line). The pressure inside the rectangular frame shown in Figure 6 was minimized using two secondary monopoles located at (0·05, 0) and (− 0·05, 0) in a pure tone diffuse primary field of 108 Hz. We observe that the minimization

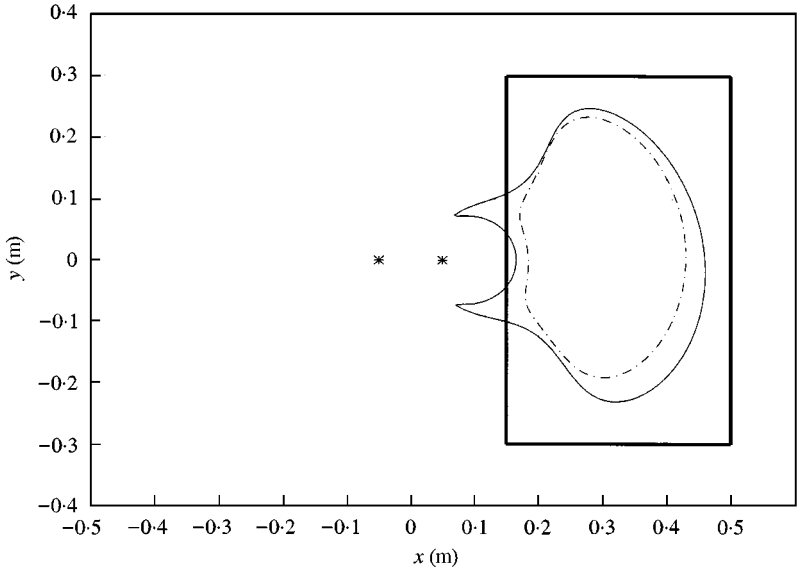

Figure 6. The 10 dB reduction contour of the average zones of quiet created by two secondary monopole sources located at positions (0·05, 0) and (− 0·05, 0) minimizing the acoustic pressure at an area represented by a bold rectangular frame, using 2-norm minimization strategy (——) and using ∞-norm minimization strategy (-·-·-·).

TABLE 1

Attenuation after control for the 2- and the ∞-norm minimization strategies

Minimization strategy	Attenuation (dB)	
	2-norm	∞-norm
2-norm	9·3	4·8
∞-norm	8·4	5·9

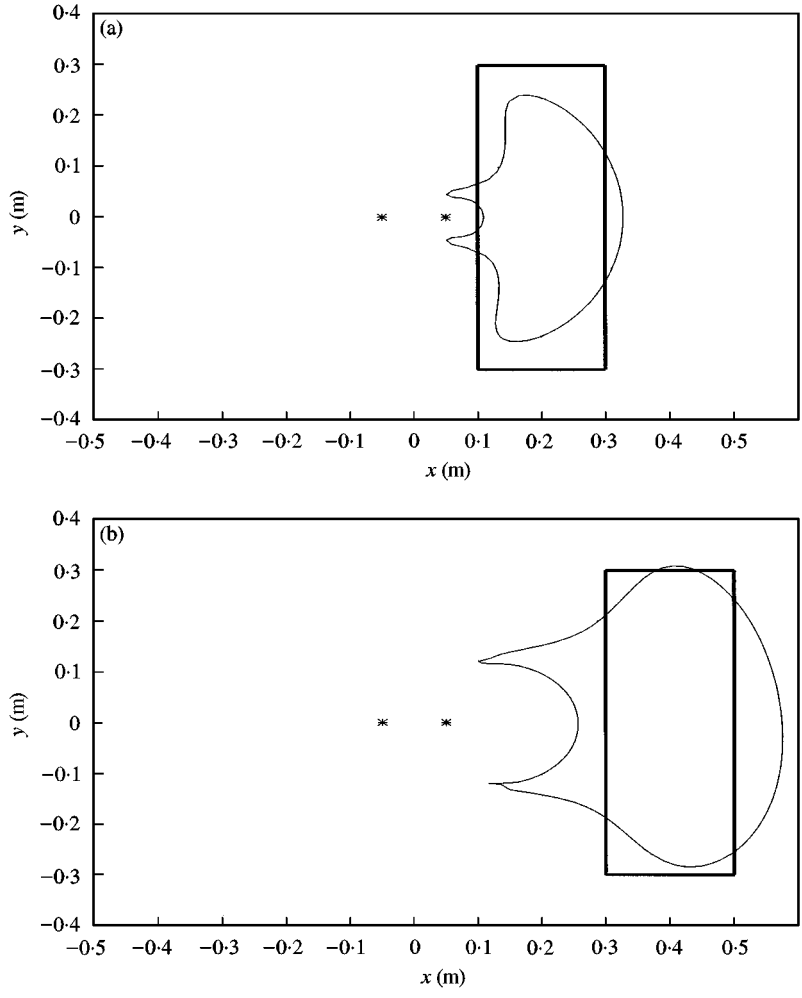

Figure 7. The 10 dB reduction contour of the average zones of quiet created by two secondary monopole sources located at positions (0·05, 0) and (− 0·05, 0), minimizing the acoustic pressure at different locations enclosed inside the rectangular frame (bold line). (a) The rectangular frame near the secondary monopoles. (b) The rectangular frame further away from the secondary monopoles.

of the acoustic pressure by using 2-norm minimization creates a larger 10 dB reduction contour than that with ∞-norm minimization. This is due to the fact that in the ∞-norm minimization the highest acoustic pressure from all the points within the minimization area is minimized. The acoustic pressure at some points within the area is difficult to control. The

extra effort required to minimize these points reduces the performance at other locations. This is in contrast to the 2-norm minimization, where the sum of squared pressure at the minimization area is minimized, and the effect of a small area on the average pressure is small. Table 1 shows that the 2-norm strategy produces 9·3 dB reduction in 2-norm of the pressure within the minimization area. However, the ∞-norm strategy produces 8·4 dB reduction in 2-norm of the pressure within the minimization area. The table also shows that the 2-norm strategy produces only 4·8 dB reduction in ∞-norm of the pressure and the ∞-norm strategy produces 5·9 dB reduction in ∞-norm of the pressure.

The effect of different minimization regions and shapes on the size of the 10 dB reduction contours created by the 2-norm minimization strategy has also been investigated in this study. Figures 7(a) and (b) show the contour lines of 10 dB reduction in the sound pressure level calculated using 2-norm minimization (solid line) for different minimization regions, as represented by the bold rectangular frames. It can be seen that the locations of the 10 dB reduction contour change with the minimization regions as expected. Figures 8(a) and (b)

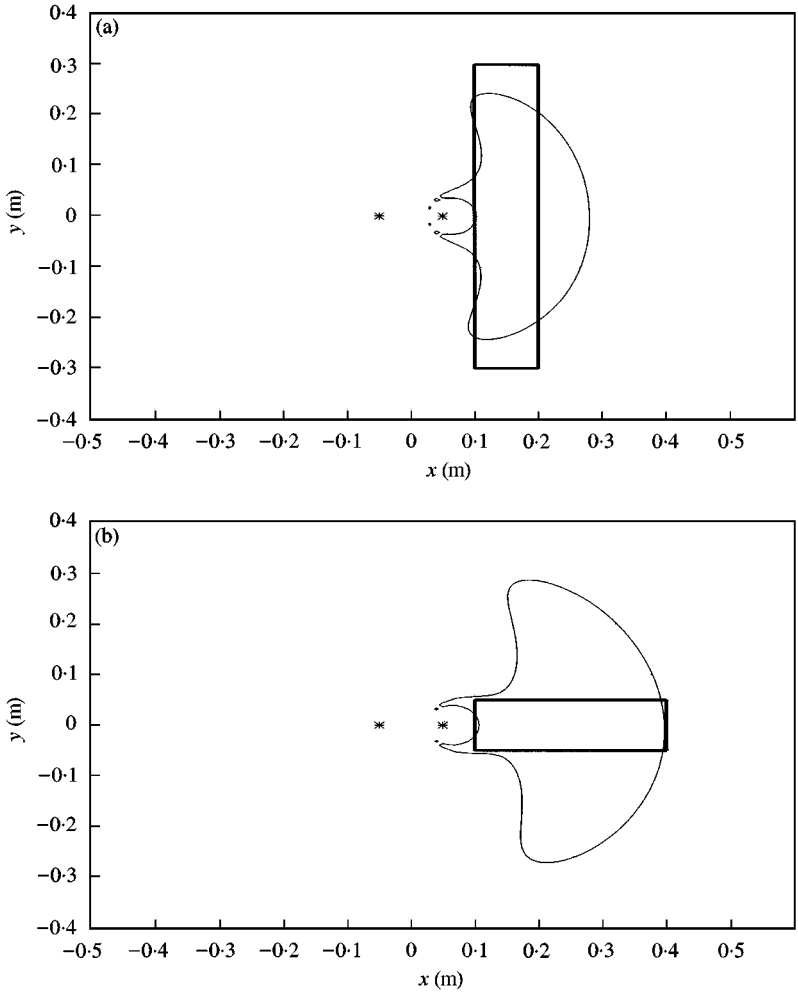

Figure 8. The 10 dB reduction contour of the average zones of quiet created by two secondary monopole sources located at positions (0·05, 0) and (− 0·05, 0) minimizing the acoustic pressure at differently shaped areas enclosed inside the rectangular frame. (a) The rectangular frame is narrow in the x-axis direction and longer in the y-axis direction. (b) The rectangular frame is narrow in the y-axis direction and longer in the x-axis direction.

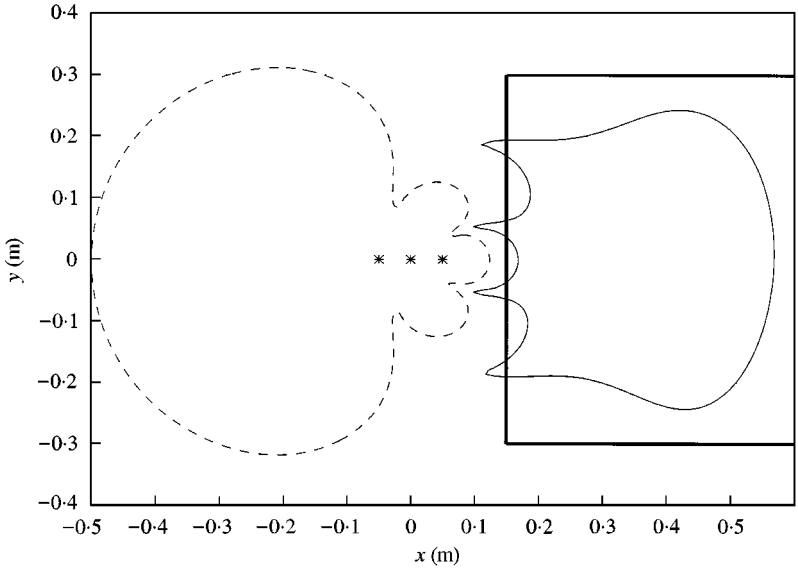

Figure 9. The 10 dB reduction contour of the average zone of quiet created by three secondary monopole sources located at positions (0, 0), (0·05, 0) and (− 0·05, 0) minimizing the acoustic pressure at an area represented by a bold rectangular frame using 2-norm minimization strategy (——), and the 10 dB increase in the primary field (- - - - -).

show the 10 dB reduction contour created by 2-norm minimization for different minimization shapes. It can be seen that the shapes of the quiet zone change with the minimization shapes. In Figure 8(a), the quiet zone has a narrow shape in x-axis direction and longer in y-axis direction similar to the minimization area. When the minimization area changes to be narrower in y-axis direction and longer in x-axis direction, the quiet zone tends to extend its size in the x-axis direction as shown in Figure 8(b). Therefore, the locations and shapes of the quiet zones can be designed using 2-norm minimization in a way which is not possible using pressure and pressure gradient cancellation.

The zone of quiet created by introducing three secondary monopoles using 2-norm minimization has also been explored. Figure 9 shows the 10 dB reduction in the pressure level (solid line) for 2-norm minimization of the pressure in an area represented by the bold rectangular frame. The three secondary monopoles are located at (0, 0), (0·05, 0) and (− 0·05, 0) represented by *, and the 10 dB amplification in the acoustic pressure of the diffuse primary field is represented by a dashed line. Figure 9 shows that three secondary monopoles create a significantly larger zone of quiet than that in the two secondary monopoles case. However, the size of the 10 dB amplification in the acoustic pressure away from the zone of quiet is also larger in this case. This shows that larger number of secondary sources provide better control over the secondary field, with the potential of producing larger zones of quiet at required locations.

5. CONCLUSIONS

In this paper, the average zones of quiet created by introducing one, two and three secondary sources using 2- and ∞-norm minimization approaches to reduce the acoustic pressure at a specified area in a tonal diffuse primary field have been explored through

computer simulations. The results have also been compared with the more traditional approaches of cancelling the acoustic pressure or the acoustic pressure and particle velocity at one point. It was shown that larger zones of quiet can be achieved with two or three secondary sources, since the secondary field is designed to better match the primary field at a large area, and not only at one point. An overall flatter secondary field and larger zone of quiet are achieved in this case. It was also shown that the ∞-norm minimization approach created a smaller zone of quiet compared to that obtained by using 2-norm minimization, due to the fact that it may focus on the more difficult points to control. The effect of different minimization locations and shapes on the zones of quiet has also been investigated in this work. It was shown that the locations and shapes of the quiet zones can be controlled by changing the minimization area.

Local active sound control using 2-norm minimization could be applied to a practical application, such as a headrest system if the sum of the mean square pressure at an array of physical microphones was minimized [1] or by using a virtual microphone approach which may not require as many microphones [17]. In a practical system, a feedback controller could be designed to control a broadband noise. This would involve optimization over both frequency and space [18]. Although only a pure tone diffuse primary field was considered in this work, the expansion of this work to broadband noise and the experimental verification of the method [19] are suggested for future study.

REFERENCES

1. P. A. Nelson and S. J. Elliott 1992 *Active Control of Sound*. London: Academic Press.
2. C. F. Ross 1980 *Ph.D. thesis, University of Cambridge, England*. Active control of sound.
3. P. Joseph 1990 *Ph.D. thesis University of Southampton, England*. Active control of high frequency enclosed sound fields.
4. P. Joseph S. J. Elliott and P. A. Nelson 1994 *Journal of Sound and Vibration* **172**, 605–627. Nearfield zones of quiet.
5. A. David and S. J. Elliott 1994 *Applied Acoustics* **41**, 63–79. Numerical studies of actively generated quiet zones.
6. M. Miyoshi, J. Shimizu and N. Koizumi 1994 *Inter-noise* **94**, 1229–1304. On arrangements of noise controlled points for producing larger quiet zones with multi-point active noise control.
7. J. Guo, J. Pan and Chaoying Bao 1997 *Journal of Acoustic Society of America* **101**, 1492–1501. Actively created quiet zones by multiple control sources in free space.
8. J. Guo and J. Pan 1995 *Proceedings of Active* **95**, 649–660. Analysis of active noise control in a free field.
9. S. Ise 1994 *Inter-noise* **94**. Theory of acoustic impedance control for active noise control.
10. J. Garcia-Bonito and S. J. Elliott 1994 *Institute of Sound and Vibration Research Memorandum* 745. Alternative strategies for actively generating quiet zones.
11. S. J. Elliott and J. Garcia-Bonito 1995 *Journal of Sound and Vibration* **186**, 696–704. Active cancellation of pressure and pressure gradient in a diffuse sound field.
12. S. Skogestad and I. Postlethwaite 1996 *Multivariable Feedback Control*. New York: John Wiley and Sons.
13. A. Gonzalez, A. Albiol and S. J. Elliott 1998 *IEEE Transactions on Speech and Audio Processing* **6**, 268–281. Minimization of the maximum error signal in active control.
14. J. Garcia-Bonito 1996 *Ph.D. thesis, University of Southampton, England*. Local active control in pure tone diffracted diffuse sound fields.
15. A. Grace 1995 *Matlab Optimisation Toolbox*. Natick, MA: The Math Works, Inc.
16. L. Vandenberghe and S. Boyd 1996 *SIAM Review* **38**, 49–95. Semidefinite programming.
17. J. Garcia-Bonito, S. J. Elliott and C. C. Boucher 1997 *ACTIVE 97*, 405–418. A novel secondary source for a local active noise control system.
18. B. Rafaely 1999 *ACTIVE 99*. Active control with optimisation over frequency and space.
19. Wen-Kung Tseng, B. Rafaly and S. J. Elliott 1999 *ACTIVE* 99. 2-norm and ∞-norm pressure minimization for local active control of sound.